

## 20.3 A 64-QAM 60GHz CMOS Transceiver with 4-Channel Bonding

Kenichi Okada, Ryo Minami, Yuuki Tsukui, Seitaro Kawai, Yuuki Seo, Shinji Sato, Satoshi Kondo, Tomohiro Ueno, Yasuaki Takeuchi, Tatsuya Yamaguchi, Ahmed Musa, Rui Wu, Masaya Miyahara, Akira Matsuzawa

Tokyo Institute of Technology, Tokyo, Japan

This paper presents the first 64QAM 60-GHz CMOS transceiver, which achieves a Tx-to-Rx EVM of -26.3dB and can transmit 10.56-Gb/s in all four channels defined in IEEE802.11ad/WiGig. By using a 4-bonded channel, 28.16-Gb/s can be transmitted in 16QAM. The front-end consumes 251mW and 220mW from a 1.2-V supply in transmitting and receiving mode, respectively.

Figure 20.3.1 shows the 60-GHz direct-conversion front-end design. The transmitter consists of a 6-stage PA, differential preamplifiers, I/Q passive mixers and a quadrature injection-locked oscillator (QILO). The receiver consists of a 4-stage LNA, differential amplifiers, I/Q double-balanced mixers, a QILO, and baseband amplifiers. A direct-conversion architecture is employed for both Tx and Rx because of wide-bandwidth capability [1]. The LO consists of the 60-GHz QILO and a 20-GHz PLL. The 60-GHz QILO works as a frequency tripler with the integrated 20-GHz PLL. It can generate 7 carrier frequencies with a 36/40-MHz reference, 58.32GHz(ch.1), 60.48GHz(ch.2), 62.64GHz(ch.3), and 64.80GHz(ch.4) defined in IEEE802.11ad/WiGig, 59.40GHz(ch.1-2), 61.56GHz(ch.2-3), and 63.72GHz(ch.3-4) for the channel bonding.

Figure 20.3.2 shows the down-conversion mixer and 3-stage baseband amplifiers on the receiver chain. For the millimeter-wave receiver design, the noise figure, linearity, gain flatness, and frequency-dependent I/Q mismatch should be considered. It is difficult to use a closed-loop baseband amplifier for improving linearity and gain flatness due to the wide bandwidth. Thus, an open-loop baseband amplifier based on the flipped voltage follower (FVF) is employed to maintain both gain flatness and linearity. The voltage gain is simply determined by the current-mirror ratio  $N$  and  $R_L/R_S$ , which contributes to improving the linearity. A mismatch in cut-off frequencies of baseband amplifiers causes the frequency-dependent I/Q phase mismatch, which is mainly caused by the low-pass characteristics of baseband amplifiers. This FVF amplifier can also relax the mismatch due to its high cut-off frequency. A current-bleeding down-conversion mixer with the capacitive cross coupling is employed to reduce the LO power and the power consumption of LO buffers. The input matching block of the LNA has a shunt-grounded structure for electrostatic discharge (ESD) protection.

Figure 20.3.3 shows the up-conversion mixer and RF differential amplifier. The wideband gain flatness and linearity are also important for the transmitter design. In this work, a mixer-first topology is employed for improving the gain flatness and linearity. An input buffer maintaining the 50- $\Omega$  impedance matching usually has a narrow-band characteristic, which degrades the gain flatness. In this design, the baseband input impedance is directly maintained by the mixer impedance. This is a known technique for the mixer-first receiver but applied to a transmitter in this work. The input impedance of the RF differential amplifier is down-converted to the baseband, and the wideband impedance flatness around 60GHz is maintained by a shunt-feedback matching technique in the RF differential amplifier [6]. A 200- $\Omega$  shunt resistor at the mixer input is also used for impedance compensation. The LO leakage can be minimized by a DC offset cancellation, which is adjusted by current sources. In addition, the mixer-first topology can relax the linearity requirement of mixer by increasing the RF path gain. Thus, the LO power for mixers can be reduced, which contributes to reducing the power consumption of I/Q LO buffers considerably, e.g., 84mW [4] becomes 37mW, even though increasing RF path gain.

Figure 20.3.4 shows the measured characteristics of the RF front-end. Both Tx and Rx cover 4 channels. The Tx conversion gain is about 15dB, excluding the PCB loss. The saturated output power is 10.3dBm at the center frequency of 61.56GHz for the 4-channel bonding. The output power is measured for both a stand-alone PA and a transceiver chip implemented on a PCB, and the PCB loss is estimated from the difference between these saturated output power depending on the frequency. The LO leakage is less than -45dBc as shown in Fig. 20.3.3. Due to the proposed up-conversion architecture, a sideband rejection ratio of more than 40dB is achieved at the 0.5-GHz offset after the I/Q calibration [5]. The Tx EVM is less than -27.1dB for

every channel and every mode, and the best Tx EVM of -29.7dB is achieved in QPSK (ch.4). The PA consumes 115mW, and the two differential amplifiers and mixers consume 16mW.

The Rx conversion gain is more than 20dB, excluding the PCB loss. SNDR at the center frequency of 61.56GHz is estimated from the measured IM3 of Rx PCB, and the measured noise figure of stand-alone LNA. A peak SNDR is 35dB excluding the PCB loss. The power consumptions of LNA, two differential amplifiers, two mixers, and two BB amplifiers are 41mW, 19mW, 23mW, and 30mW, respectively. The phase noise measured at Tx output is -96.5dBc/Hz@1MHz-offset at the center frequency of 61.56GHz. The measured free-running frequency of QILO is from 58 to 66GHz. The 20-GHz PLL consumes 64mW. QILOs for Tx and Rx consume 18mW and 15mW, and I/Q LO buffers consume 37mW and 28mW, respectively. Both QILO and LO buffers can be turned off in TDD operation.

Figure 20.3.5 shows the measured constellation and performance summary. Two PCBs are used. One is for Tx mode and the other is for Rx mode with on-board 36-MHz TXCOs. Single-carrier modulated I/Q signals are generated by an arbitrary waveform generator (Tektronix AWG70002A) with symbol rates of 1.76GS/s (for 1 channel) and 7.04GS/s (for 4-bonded channel), and a roll-off factor of 25%. The spectrum is measured with a spectrum analyzer and a down-conversion mixer, which satisfies the IEEE802.11ad spectrum mask for every channel. An oscilloscope (Tektronix DSA73304D) is used to evaluate the constellation and EVM. The measured Tx-to-Rx EVM ( $-SNR$ ) in 64QAM is less than -24dB at least for every channel with an RF data rate of 10.56Gb/s, and -26.3dB is achieved at channel 4. The phase noise has the largest influence on the EVM performance in this design. By using the 4-bonded channel, 14.08Gb/s in QPSK and 28.16Gb/s in 16QAM have been achieved within a BER of  $10^{-3}$  (EVM is less than -9.8dB and -16.5dB at least). The maximum communication distances with 14-dBi horn antennas, within an EVM of -9.8dB, -16.5dB, and -22.5dB, are 2.4m, 2.0m, 2.6m, and 0.9m in QPSK, 0.7m, 0.6m, 0.6m, and 0.4m in 16QAM, 0.08m, 0.08m, 0.13m, and 0.06m in 64QAM for channels 1 to 4, respectively.

Figure 20.3.6 shows a comparison table for 60-GHz CMOS transceivers [1-9]. This paper reports the first 64QAM 60GHz transceiver with a 28.16-Gb/s wireless data rate.

Figure 20.3.7 shows the die photo. The transceiver is fabricated in a 65-nm CMOS technology. The core areas of the transmitter, receiver, PLL and control logic are 1.035mm<sup>2</sup>, 1.25mm<sup>2</sup>, 0.90mm<sup>2</sup>, and 0.67mm<sup>2</sup>, respectively.

### Acknowledgments:

This work was partially supported by MIC, MEXT, STARC, Canon Foundation, and VDEC in collaboration with Cadence Design Systems, Inc., and Agilent Technologies Japan, Ltd. The authors thank Dr. Hirose, Dr. Suzuki, Dr. Sato, and Dr. Kawano of Fujitsu Laboratories, Ltd., and Prof. Ando of Tokyo Institute of Technology for their valuable discussions and technical supports.

### References:

- [1] K. Okada, *et al.*, "A 60GHz 16QAM/8PSK/QPSK/BPSK direct-conversion transceiver for IEEE802.15.3c," *ISSCC Dig. Tech. Papers*, pp. 160-161, Feb. 2011.
- [2] A. Siliqaris, *et al.*, "A 65nm CMOS fully integrated transceiver module for 60GHz wireless HD applications," *ISSCC Dig. Tech. Papers*, pp. 162-163, Feb. 2011.
- [3] S. Emami, *et al.*, "A 60GHz CMOS phased-array transceiver pair for multi-Gb/s wireless communications," *ISSCC Dig. Tech. Papers*, pp. 164-165, Feb. 2011.
- [4] K. Okada, *et al.*, "A full 4-channel 6.3Gb/s 60GHz direct-conversion transceiver with low-power analog and digital baseband circuitry," *ISSCC Dig. Tech. Papers*, pp. 218-219, Feb. 2012.
- [5] S. Kawai, *et al.*, "A digitally-calibrated 20-Gb/s 60-GHz direct-conversion transceiver in 65-nm CMOS," *RFIC Symp.*, pp. 137-140, June 2013.
- [6] V. Vidjokovic, *et al.*, "A low-power 57-to-66GHz transceiver in 40nm LP CMOS with -17dB EVM at 7Gb/s," *ISSCC Dig. Tech. Papers*, pp. 268-269, Feb. 2012.
- [7] T. Mitomo, *et al.*, "A 2Gb/s-throughput CMOS transceiver chipset with in-package antenna for 60GHz short-range wireless communication," *ISSCC Dig. Tech. Papers*, pp. 266-267, Feb. 2012.
- [8] V. Vidjokovic, *et al.*, "A low-power radio chipset in 40nm LP CMOS with beamforming for 60GHz high-data-rate wireless communication," *ISSCC Dig. Tech. Papers*, pp. 236-237, Feb. 2013.
- [9] T. Tsukizawa, *et al.*, "A fully integrated 60GHz CMOS transceiver chipset based on WiGig/IEEE802.11ad with built-in self calibration for mobile applications," *ISSCC Dig. Tech. Papers*, pp. 230-231, Feb. 2013.

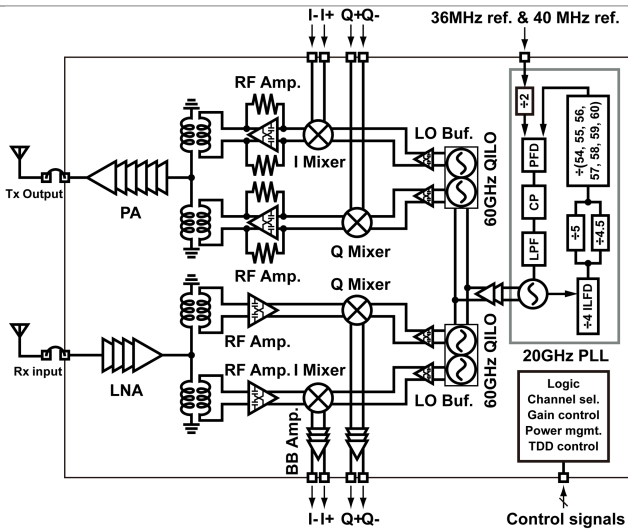


Figure 20.3.1: Block diagram of the 60-GHz direct-conversion transceiver.

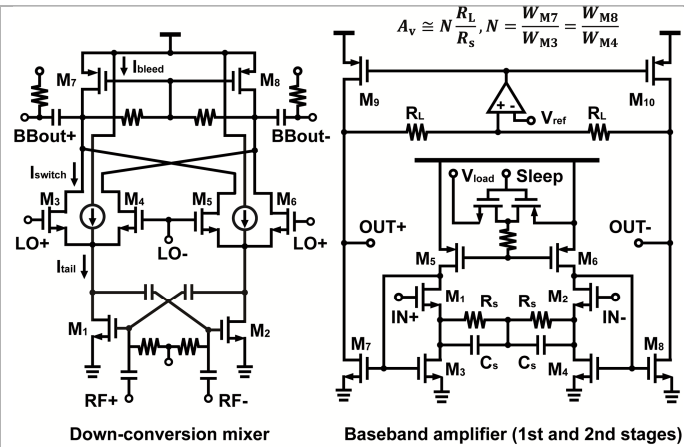


Figure 20.3.2: Receiver blocks.

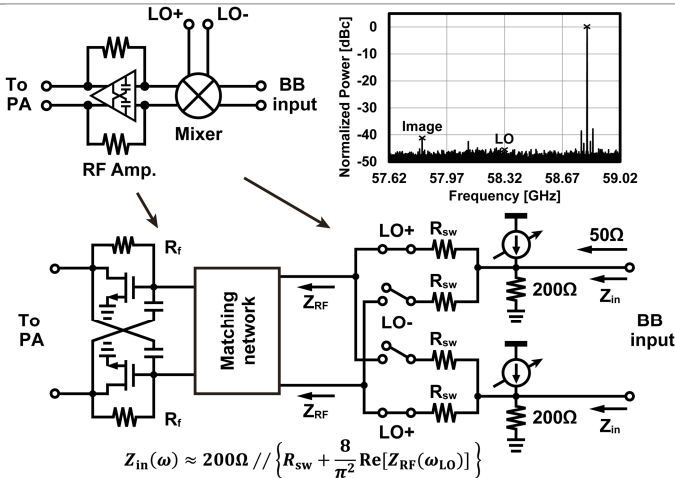


Figure 20.3.3: Transmitter blocks of mixer-first topology.

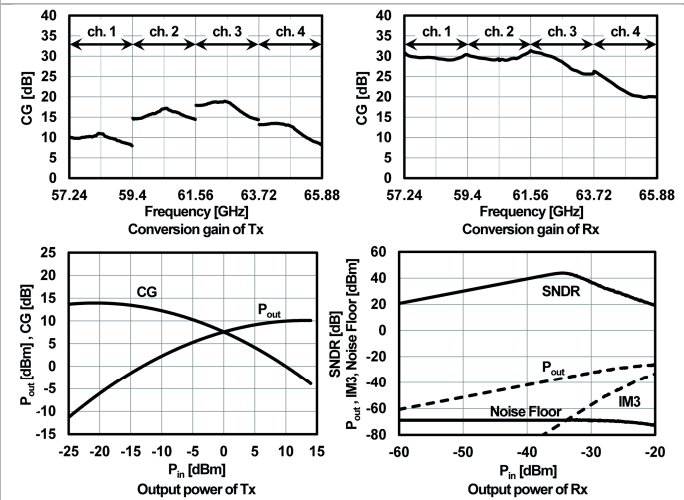


Figure 20.3.4: Measured characteristics of RF front-end.

| Channel/<br>Carrier<br>freq. | ch.1<br>58.32GHz | ch.2<br>60.48GHz | ch.3<br>62.64GHz | ch.4<br>64.80GHz | ch.1-ch.4<br>Channel bond |
|------------------------------|------------------|------------------|------------------|------------------|---------------------------|
| Modulation                   | 64QAM            |                  |                  |                  | 16QAM                     |
| Data rate*                   | 10.56Gb/s        | 10.56Gb/s        | 10.56Gb/s        | 10.56Gb/s        | 28.16Gb/s                 |
| Constellation**              |                  |                  |                  |                  |                           |
| Spectrum**                   |                  |                  |                  |                  |                           |
| Tx EVM**                     | -27.1dB          | -27.5dB          | -28.0dB          | -28.8dB          | -20.0dB                   |
| Tx-to-Rx<br>EVM***           | -24.6dB          | -23.9dB          | -24.4dB          | -26.3dB          | -17.2dB                   |

LO (20GHz PLL + 60GHz QILO)

|                          |  |
|--------------------------|--|
| Frequency                | 58.32-64.80GHz (1.08GHz-step)  |
| QILO range               | 58-66GHz   |
| Phase noise @1MHz-offset | -95.3dBc/Hz (ch.1), -93.8dBc/Hz (ch.2), -92.1dBc/Hz (ch.3), -95.7dBc/Hz (ch.4) |

Figure 20.3.5: Measured constellation and performance summary.

|                   | Data rate /<br>Modulation            | Tx-to-Rx<br>EVM | Integration   | Power consumption                      |
|-------------------|--------------------------------------|-----------------|---|--|
| Tokyo Tech [1]    | 11Gb/s(16QAM)                        | -17dB           | 65nm, direct-conversion, Tx, Rx, LO, antenna                      | Tx: 186mW<br>Rx: 106mW<br>PLL: 66mW    |
| CEA-LETI [2]      | 3.8Gb/s(16QAM)                       | -18dB           | 65nm, heterodyne, Tx, Rx, LO, antenna                             | Tx: 1,357mW<br>Rx: 454mW               |
| SiBeam [3]        | 7.14Gb/s(16QAM)                      | -19dB           | 65nm, 32x32-array heterodyne, Tx, Rx, LO                          | Tx: 1,820mW<br>Rx: 1,250mW             |
| Tokyo Tech [4, 5] | 16Gb/s(16QAM)<br>20Gb/s(16QAM)[5]    | -21dB           | 65nm, direct-conversion, Tx, Rx, LO, antenna, analog & digital BB | Tx: 319mW<br>Rx: 223mW                 |
| IMEC [6]          | 7Gb/s(16QAM)                         | -18dB           | 40nm, direct-conversion, Tx, Rx, w/o PLL                          | Tx: 167mW<br>Rx: 112mW                 |
| Toshiba [7]       | 2.62Gb/s(QPSK)                       | N/A             | 65nm, heterodyne, Tx, Rx, LO, antenna, analog & digital BB        | Tx: 160mW<br>Rx: 233mW                 |
| IMEC [8]          | 7Gb/s(16QAM)                         | -15dB           | 40nm, 4-array direct-conversion, Tx, Rx, LO, antenna              | Tx: 330mW<br>Rx: 284mW<br>for 1 stream |
| Panasonic [9]     | 2.5Gb/s(QPSK)                        | -22dB           | 90nm, direct-conversion, Tx, Rx, LO, antenna, analog & digital BB | Tx: 347mW<br>Rx: 274mW                 |
| This work         | 10.56Gb/s(64QAM)<br>28.16Gb/s(16QAM) | -26dB           | 65nm, direct-conversion, Tx, Rx, LO                               | Tx: 251mW<br>Rx: 220mW                 |

Figure 20.3.6: Performance comparison of 60-GHz CMOS transceiver.

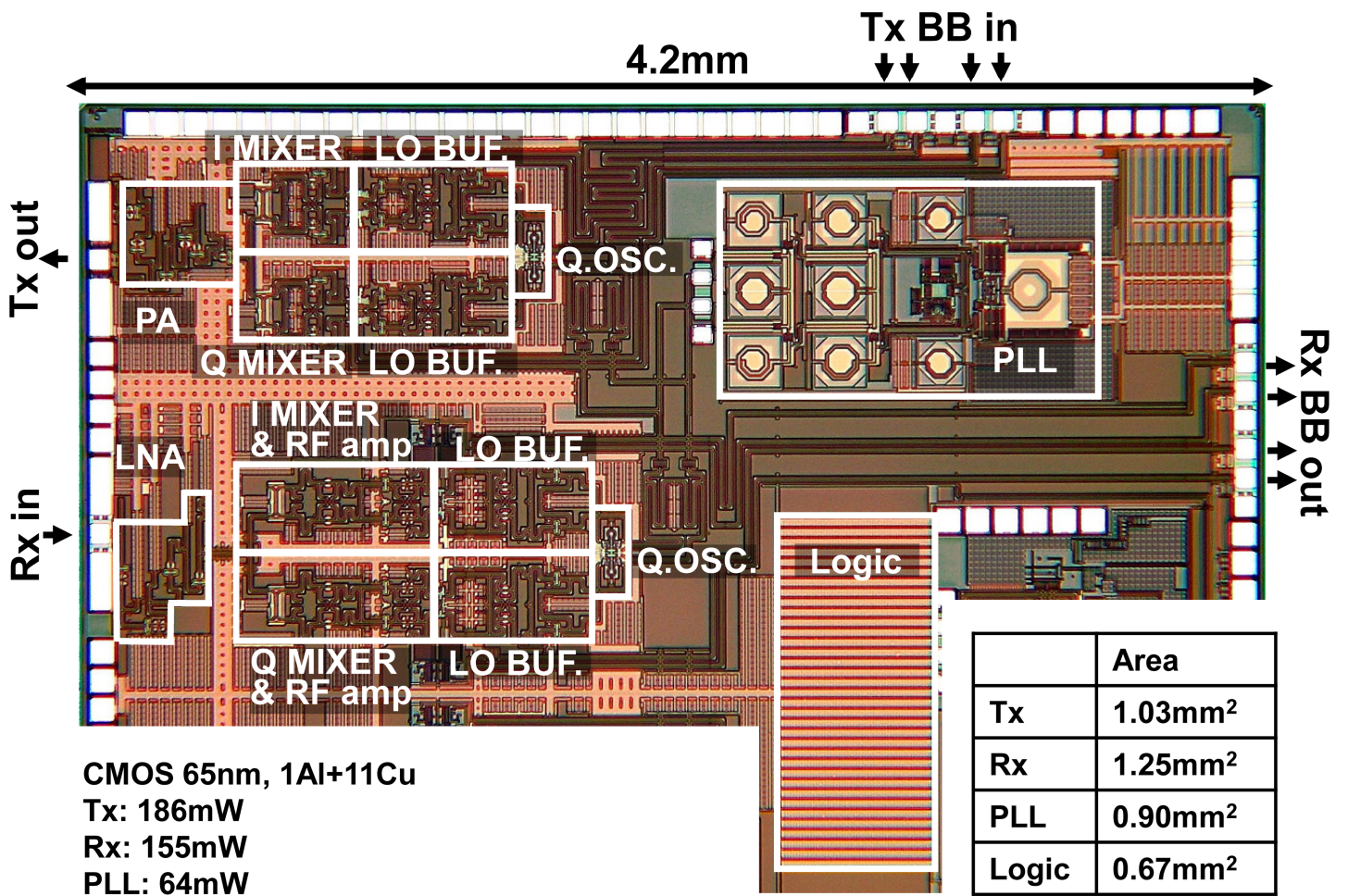


Figure 20.3.7: Die micrograph.